

RC 201-21 C2

STIC-ILL

From: Loeb, Bronwen
Sent: Sunday, January 26, 2003 10:20 PM
To: STIC-ILL
Subject: ILL order 10/019,586

Chishima, T. et al. Cancer Research (1997) 57:2042-2047

(for lack of unity)

Bronwen Loeb, PhD

AU 1636
703-605-1197
CM1 11B-15
Mailbox 11E-12

Cancer Invasion and Micrometastasis Visualized in Live Tissue by Green Fluorescent Protein Expression

Takashi Chishima, Yohei Miyagi, Xiaoen Wang, Hiroyuki Yamaoka, Hiroshi Shimada, A. R. Moossa, and Robert M. Hoffman¹

Departments of Surgery [T. C., H. Y., H. S.] and Pathology [Y. M.], Yokohama City University School of Medicine, Yokohama, Japan; Department of Surgery, University of California, San Diego, California 92103-8220 [T. C., H. Y., A. R. M., R. M. H.]; and AntiCancer, Inc., San Diego, California 92111 [X. W., R. M. H.]

ABSTRACT

We report the establishment of stable, high-level green fluorescent protein (GFP)-expressing cell lines *in vitro* that permit the detection and visualization of distant micrometastases when they are implanted orthotopically in nude mice. Chinese hamster ovary cells were transfected with the dicistronic expression vector containing the humanized GFP cDNA. A stable GFP-expressing clone was selected in 1.5 μ M methotrexate *in vitro* and injected s.c. in nude mice. Stable high-level expression of GFP was maintained in the s.c. growing tumors. To use GFP expression for metastasis studies, fragments of s.c. growing tumor, which are comprised of GFP-expressing cells, were implanted by surgical orthotopic implantation in the ovary of nude mice. Subsequent micrometastases were detected in systemic organs and could be visualized by GFP fluorescence in the lung, liver, and other organs down to the single-cell level. With this fluorescent tool, we detected and visualized for the first time tumor cells at the microscopic level in fresh viable tissue in their normal host organ. Confocal microscopy further enabled us to study physiologically relevant patterns of invasion and micrometastasis.

INTRODUCTION

Our understanding of the cancer metastatic process has advanced considerably in recent years. However, the early stages of tumor progression and micrometastasis formation have been difficult to analyze and have been hampered by the inability to identify small numbers of tumor cells against a background of many host cells. The visualization of tumor cell emboli, micrometastases, and their progression over real-time during the course of the disease models has not been easy to study in current models of metastasis. Previous studies used transfection of tumor cells with the *Escherichia coli* β -galactosidase (*lacZ*) gene to detect micrometastases (1, 2). However, detection of *lacZ* requires extensive histological preparation; therefore, it is impossible to detect and visualize tumor cells in viable fresh tissue at the microscopic level. The visualization of tumor invasion and micrometastasis formation in viable fresh tissue is necessary for a critical understanding of tumor progression and its control.

To enhance the resolution of the visualization of micrometastases in fresh tissue, we have used the *GFP*² gene, cloned from the bioluminescent jellyfish *Aequorea victoria* (3). GFP has demonstrated its potential for use as a marker for gene expression in a variety of cell types (4, 5). The GFP cDNA encodes a 283-amino acid polypeptide with a molecular weight of M_r 27,000 (6, 7). The monomeric GFP requires no other *Aequorea* proteins, substrates, or cofactors to fluoresce (8). Recently, GFP gene gain-of-function mutants have been generated by various techniques (9-12). For example, the GFP-S65T clone has the serine 65 codon substituted with a threonine codon that

results in a single excitation peak at 490 nm (9). Moreover, to develop higher expression in human and other mammalian cells, a humanized hGFP-S65T clone was isolated (13). The much brighter fluorescence in the mutant clones allows for easy detection of GFP expression in transfected cells.

We demonstrate in this report the isolation of stable transfectants of CHO cells that express GFP *in vitro*. The stable transfectants are highly fluorescent *in vivo* in tumors formed from the injected cells. Using these cells and an orthotopic metastatic model that allows for spontaneous metastasis in nude mice, the high-level expression of GFP enables the detection and visualization of distant micrometastases in their normal target organs such as in the lung and liver, that otherwise would go undetected in live tissue. These results suggest that GFP gene-transfected tumor cells represent a powerful new tool for understanding tumor cell dissemination and progression at their earliest stages.

MATERIALS AND METHODS

DNA Manipulations and Expression Vector Constructions. The dicistronic expression vector (pED-mtx¹) was obtained from Genetics Institute (Cambridge, MA; Ref. 14). The expression vector containing the codon-optimized hGFP-S65T gene was purchased from Clontech Laboratories, Inc. (Palo Alto, CA). To construct the hGFP-S65T-containing expression vector, phGFP-S65T was digested with *Hind*III, blunted at the end. The entire hGFP coding region was then excised with *Xba*I. The pED-mtx¹ vector was digested with *Pst*I, blunted at the end, and further digested with *Xba*I. The hGFP-S65T cDNA fragment was then unidirectionally subcloned into pED-mtx¹.

Cell Culture, Transfection, and Subcloning. CHO-K1 cells were cultured in DMEM (Life Technologies, Inc.) containing 10% FCS (Gemini Bio-products, Calabasas, CA), 2 mM L-glutamine, and 100 μ M nonessential amino acids (Irvine Scientific, Santa Ana, CA). For transfection, near-confluent CHO-K1 cells were incubated with a precipitated mixture of LipofectAMINE reagent (Life Technologies, Inc.) and saturating amounts of plasmids for 6 h before being replenished with fresh medium. CHO-K1 cells were harvested by trypsin/EDTA 48 h after transfection and subcultured at a ratio of 1:15 into selective medium that contained 1.5 μ M MTX. Cells with stably integrated plasmids were selected by growing transiently transfected cells in the MTX-containing medium. Clones were isolated with cloning cylinders (Bel-Art Products, Pequannock, NJ) by trypsin/EDTA. They were amplified and transferred with conventional culture methods. Clone-38 was chosen because of its high-intensity GFP fluorescence and stability.

Doubling Time of Stable GFP Clones. CHO-K1 parental cells and Clone-38 cells were seeded at 2.0×10^5 in 60-mm culture dishes. The cells were harvested and counted every 24 h using a hemocytometer (Reichert Scientific Instruments, Buffalo, NY). The doubling time was calculated from the cell growth curve over 6 days.

Tumor Growth. Three 6-week-old BALB/c nu/nu female mice were injected s.c. with a single dose of 10^7 Clone-38 cells. Cells were first harvested by trypsinization and washed three times with cold serum-containing medium and then kept on ice. Cells were injected in a total volume of 0.4 ml within 40 min of harvesting. The nude mice were sacrificed to harvest the tumor fragments 3 weeks after tumor cell injection.

Orthotopic Implantation and Analysis of the Metastases. Tumor fragments (1 mm³) derived from the nude mouse s.c. Clone-38 tumor were

Received 12/17/96; accepted 4/1/97

The costs of publication of this article were defrayed in part by the payment of page charges. This article must therefore be hereby marked advertisement in accordance with 18 U.S.C. Section 1734 solely to indicate this fact.

¹ To whom requests for reprints should be addressed, at AntiCancer, Inc., 7917 Ostrow St., San Diego, CA 92111. Phone: (619) 654-2555; Fax: (619) 268-4175.

² The abbreviations used are: GFP, green fluorescent protein; CHO, Chinese hamster ovary; MTX, methotrexate; DHFR, dihydrofolate reductase.

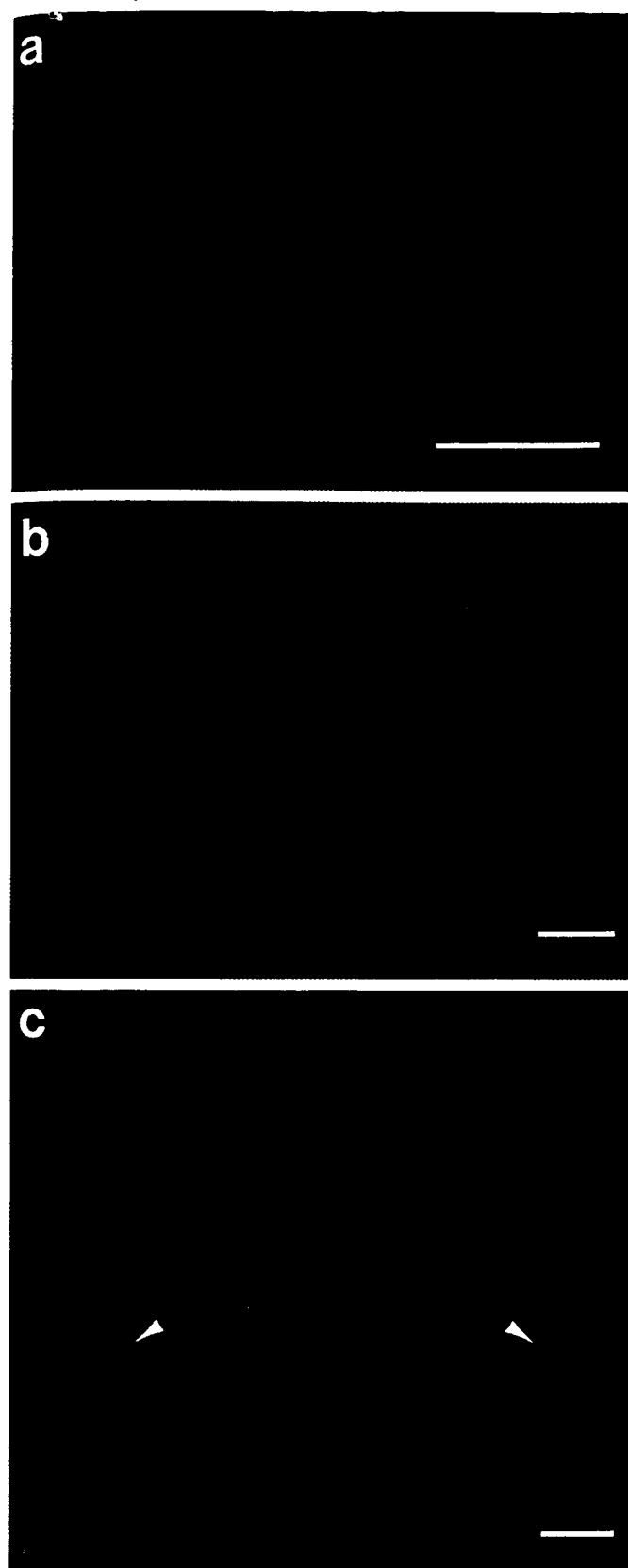


Fig. 1. Stable high-level expression GFP transfectants *in vitro* and *in vivo*. Bars, 200 μ m. a, GFP stable expression cell line CHO-K1-GFP 38 (Clone-38). CHO cells were transfected with the pED-mtx^r vector in which the *hGFP-S65T* and *DHFR* genes were transcribed in a dicistronic message. The stable high expression Clone-38 was selected in 1.5 μ M MTX. b, GFP-expressing s.c. tumor in nude mouse formed from Clone-38. The tumor was harvested when the tumor had reached approximately 15 mm in diameter. Fresh tumor tissue was smeared on slides. c, surgical orthotopic implantation of GFP

implanted by surgical orthotopic implantation on the ovarian serosa in six nude mice (15). The mice were anesthetized by isoflurane inhalation. An incision was made through the left lower abdominal pararectal line and peritoneum. The left ovary was exposed, and part of the serosal membrane was scraped with forceps. Four 1-mm³ tumor pieces were fixed on the scraped site of the serosal surface with an 8-0 nylon suture (Look, Norwell, MA). The ovary was then returned into the peritoneal cavity, and the abdominal wall and the skin were closed with 6-0 silk sutures. Four weeks later, the mice were sacrificed, and the lungs and the other organs were removed. The fresh samples were sliced at approximately 1-mm thickness and observed directly under fluorescence and confocal microscopy. The samples were also processed for histological examination for fluorescence in frozen sections. The slides were then rinsed with PBS and then fixed for 10 min at 4°C in 2% formaldehyde plus 0.2% glutaraldehyde in PBS. The slides were washed with PBS and stained with H&E using standard techniques.

Stability of GFP Expression. The s.c. Clone-38 tumors from the nude mice were minced for *in vitro* culture. Cells were subcloned in the cell culture medium in the absence of MTX and termed Clone-38 nude. Parental Clone-38 cells (10⁷) maintained in 1.5 μ M MTX and Clone-38 nude cells maintained in the absence of MTX were harvested. Cell extracts were prepared by lysis in 0.1% IGEPAL CA-630 (Sigma Chemical Co.) with 1 mM EDTA in PBS. The cell extracts were diluted 1:10 with PBS. GFP fluorescence was measured with a fluorescence photometer (Hitachi F-2000; excitation 490 nm, emission 515 nm).

Sensitivity of Detection of GFP Transfectants. Clone-38 cells (5×10^6) were injected into a nude mouse through the tail vein. After 2 min, the mouse was sacrificed, and fresh visceral organs were analyzed by fluorescence microscopy.

Microscopy. Light and fluorescence microscopy were carried out using a Nikon microscope equipped with a Xenon lamp power supply and a GFP filter set (Chromatechnology Corp., Brattleboro, VT). The confocal microscopy system was an MRC-600 confocal imaging system (Bio-Rad) mounted on a Nikon microscope with an argon laser.

RESULTS

Isolation of Stable High-Level Expression GFP Transfectants of CHO-K1 Cells. The expression vector-transfected cells were able to grow in levels of MTX up to 1.5 μ M. The selected MTX-resistant CHO cells had a striking increase in GFP fluorescence compared to the transiently transfected cells. A subclone was termed CHO-K1 GFP 38 (Clone-38; Fig. 1a), which proved to be stable in 1.5 μ M MTX, possibly due to stable chromosomal integration of the amplified *GFP* genes. There was no difference in the cell proliferation rates of parental cells and selected transfectants determined by comparing their doubling times (Table 1).

Table 1 Doubling times of parental CHO and GFP-transfected CHO cells

Cell lines	Doubling time \pm SD (h) ^a
Parental CHO cells	21.2 \pm 4.5
GFP-transfected Clone-38 cells	25.2 \pm 3.0

^a Mean of three assays \pm SD ($P = 0.269$).

Table 2 GFP fluorescence of CHO Clone-38 cells grown *in vitro* and *in vivo*

Cell lines	Fluorescence units ^a
Clone-38 <i>in vitro</i>	500.1 \pm 30.3
Clone-38 from SCID nude mice	476.6 \pm 25.2

^a Mean of four assays \pm SD ($P = 0.278$).

expressing Clone-38 tumor in the ovary of a nude mouse. Four 1-mm³ fragments of the s.c.-grown Clone-38 tumor, described in Fig. 1b, were implanted to the left ovary of nude mice by surgical orthotopic implantation. The primary tumor formed with well-developed vessels (arrowheads) and intense expression of GFP.

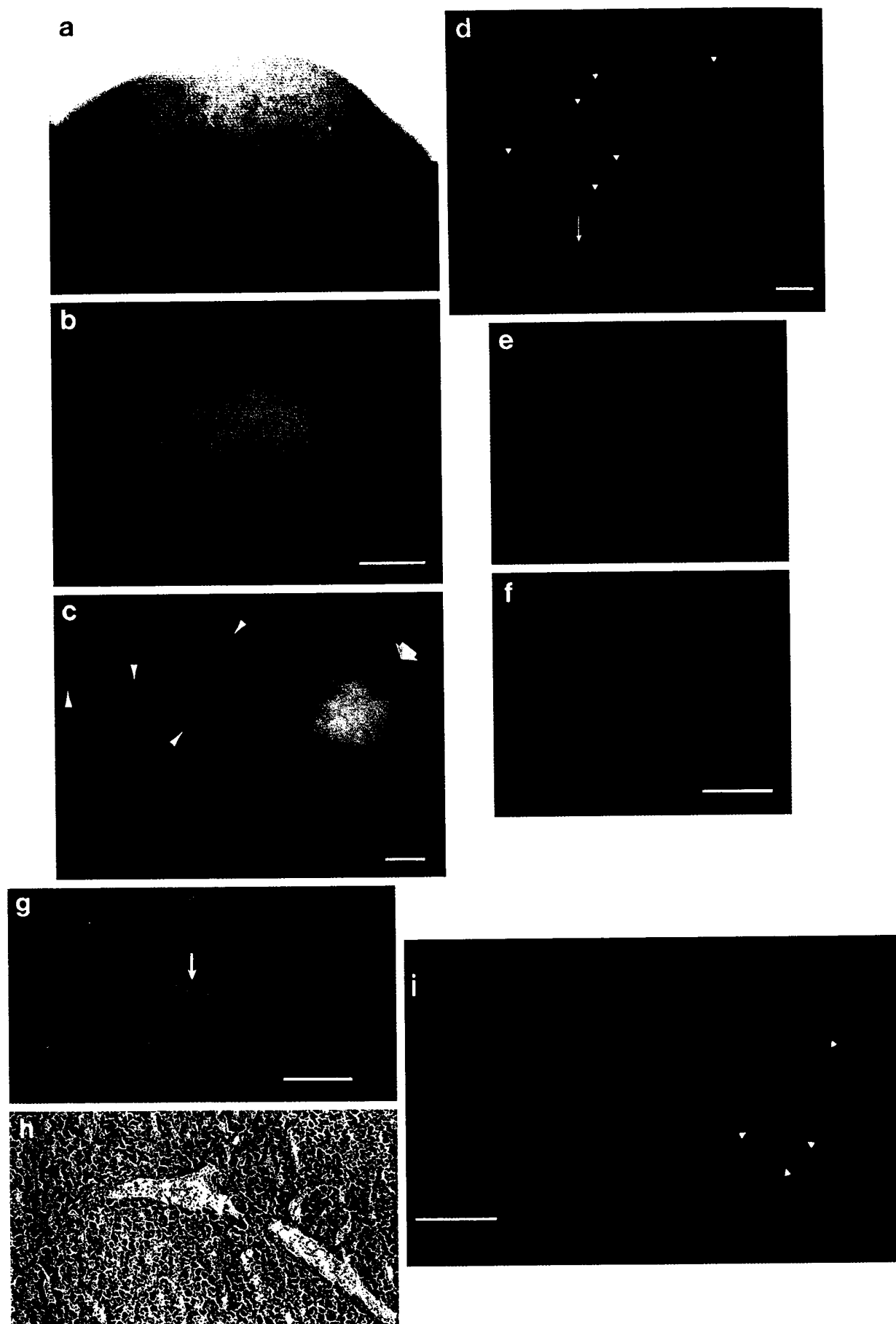


Fig. 3. To st
fectants in
after tail v
organ tiss
observed
treatment
expressin
and c. GF
boli in a c
in the hej

Sta
Nude
were
13.0
strong

Fig
remov
of Clo
metast
the nu
bright
single
pleur
mem
thick
in sp
visu
wer
(cen
fror

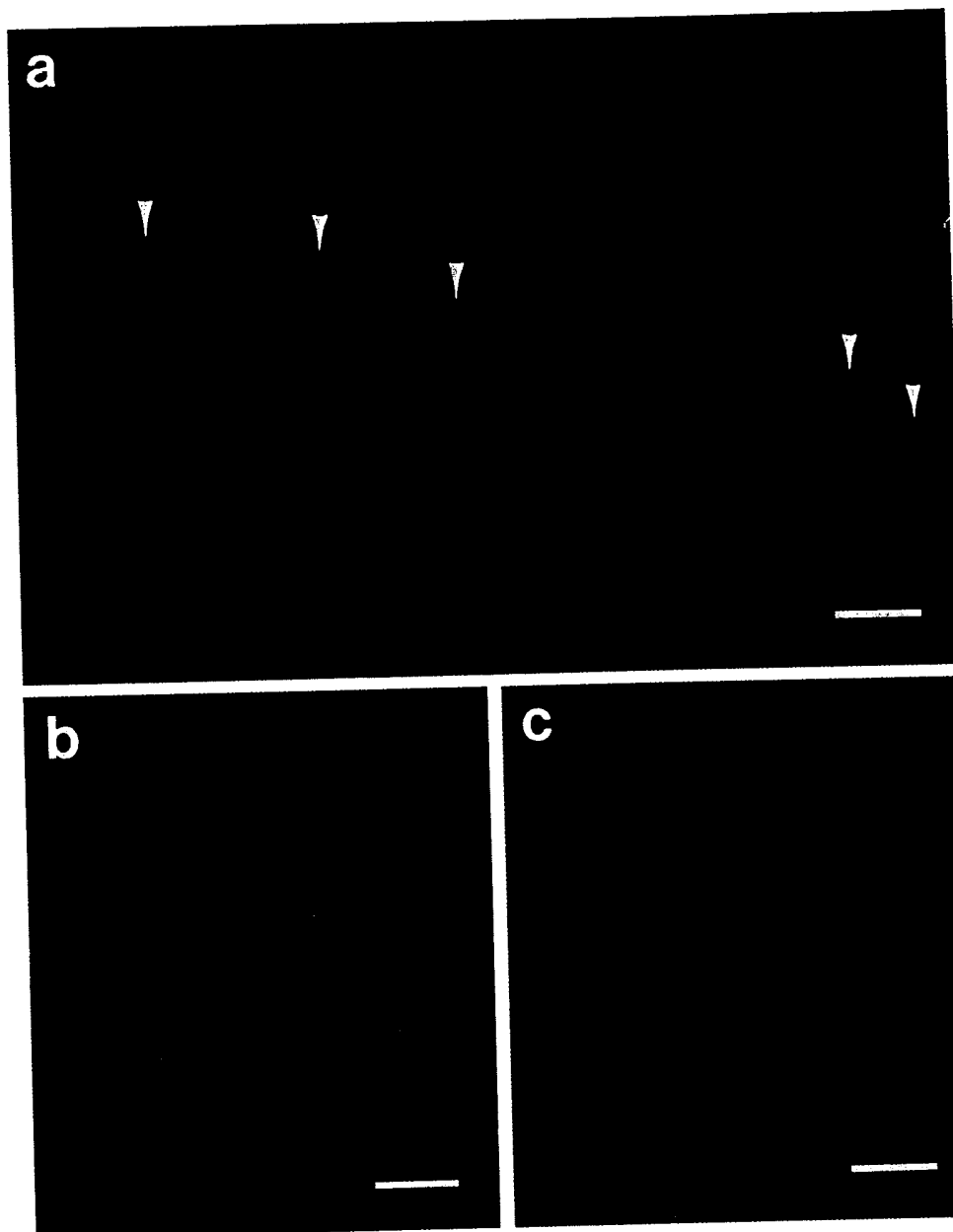


Fig. 3. GFP transfectants in veins and capillaries. To study the limit of detection of GFP transfectants *in vivo*, a nude mouse was sacrificed 2 min after tail vein injection of Clone-38 cells. The fresh organ tissues removed from the mice were directly observed under fluorescence microscopy with no treatment. Bars, 100 μ m. *a*, arrowheads, GFP-expressing Clone-38 cells in a peritoneal vessel. *b* and *c*, GFP-expressing Clone-38 cells formed embolus in a capillary of the right adrenal gland (*b*) and in the hepatic vein (*c*).

Stable High-Level Expression of GFP in CHO Tumors in Nude Mice. Three weeks after injection of Clone-38 cells, the mice were sacrificed. All mice had a s.c. tumor that ranged in diameter from 13.0 to 18.5 mm (mean, 15.2 mm \pm 2.9). The tumor tissue was strongly fluorescent, thereby demonstrating stable, high-level GFP

expression *in vivo* during tumor growth (Fig. 1*b*). No obvious metastases were found in systemic organs. GFP was extracted from Clone-38 cells and Clone-38 nude cells subcloned from the tumor formed from Clone-38 cells. The extraction experiments showed that GFP expression of the transfectants did not decrease *in vivo*, even in

Fig. 2. GFP-expressing macro- and micrometastases in nude mice that were orthotopically implanted with 1-mm³ cubes of Clone-38 tumor into the ovary in Fig. 1*c*. The fresh organ tissues removed from the mice were directly observed under fluorescence microscopy with no treatment (*a-f*). Bars: *b*, *c*, and *d*, 200 μ m; *f*, *g*, and *i*, 100 μ m. *a*, lung metastasis (870 μ m in diameter) of Clone-38. The entire fresh lung was observed under the microscope. The tumor was detected grossly under bright-field microscopy. *b*, GFP-expressing lung metastasis of Clone-38. The metastatic lesion pictured in *a* was viewed by fluorescence microscopy. This metastasis had strong GFP expression. *c*, micrometastasis of lung viewed by fluorescence in viable tissue. Note the numerous GFP-fluorescent micrometastases (15–75 μ m; arrowheads) around the main metastatic lesion (arrow) pictured in *a* and *b*. Most of the micrometastases could not be seen under bright-field microscopy (data not shown). *d*, GFP-fluorescent micrometastases infiltrating the contralateral ovary. Arrow, developing micrometastasis. Also many micrometastases, at the single-cell level (<10 μ m), were visualized at their earliest stage in the whole ovary (arrowheads). *e*, surface of fresh pleural membrane in mouse. No metastatic lesion was detected on the pleural membrane under bright-field microscopy. *f*, same fields as *d* under fluorescence microscopy. Many GFP-fluorescent micrometastases (5–80 μ m) could be detected on the pleural membrane at the single-cell level. *g*, micrometastasis (70 μ m) in the liver was shown by a green color (arrow). The sample was processed for histological examination in frozen sections (5- μ m thick). The metastatic lesion was easily detected and visualized by GFP fluorescence shown by green color. GFP fluorescence is easily distinguished from the yellow autofluorescence that occurs in specimens fixed by drying on the slide. *h*, the metastatic lesion pictured in *h* was stained by H&E. Compared with fluorescence microscopy, the metastatic lesion is difficult to detect and visualize. *i*, micrometastasis in the lung at the earliest stage visualized with confocal microscopy. The fresh lung tissue was sliced at approximately 1-mm thickness. Several sizes of colony were selected for observation from the fresh lung tissue of a nude mouse at a single point. In the small colony (left; 25 μ m), the packing density of tumor cells was tight. In the medium colony (center, 72 μ m), tumor cells were still growing tightly. In the large colony (right; 190 μ m), the packing density of tumor cells decreased in the center of the colony. Some cells were detached from the primary tumor and spread into lung tissue.

the absence of MTX, as determined by fluorescence spectrometry (Table 2).

GFP-expressing Macro- and Micrometastases in Nude Mice.

Six nude mice were implanted with 1-mm³ cubes of Clone-38 tumor into the ovary and were sacrificed at 4 weeks. All mice had tumors in the ovaries ranging in diameter from 18.7 to 25.3 mm (mean, 21.9 ± 3.1 mm). The tumor had also seeded throughout the peritoneal cavity, including the colon (six of six mice), cecum (five of six), small intestine (four of six), spleen (one of six), and peritoneal wall (six of six). The primary tumor and peritoneal metastases were strongly fluorescent (Fig. 1c). Numerous micrometastases were detected by fluorescence on the lungs of all mice (Fig. 2, a–c). Multiple micrometastases were also detected by fluorescence on the liver (one of six), kidney (one of six), contralateral ovary (three of six), adrenal gland (two of six), para-aortic lymph node (five of six), and pleural membrane (five of six) at the single-cell level (Fig. 2, d and f). These single-cell micrometastases could not be detected by standard histological techniques. Fig. 2, g and h, demonstrate micrometastasis in the liver. Even these multiple-cell small colonies were difficult to detect by H&E staining, but they could be detected and visualized clearly by GFP fluorescence. Some colonies were observed under confocal microscopy. As these colonies developed, the density of tumor cells were markedly decreased in the center of the colonies (Fig. 2i).

High Resolution Visualization of GFP-expressing Micrometastasis *in Vivo*. GFP transfectants injected via the tail vein were detected and visualized in the peritoneal wall vessels (Fig. 3a). These cells formed emboli in the capillaries of the lung, liver, kidney, spleen, ovary, adrenal gland, thyroid gland, and brain (Fig. 3, b and c).

DISCUSSION

We have demonstrated the effectiveness and sensitivity of the *GFP* gene as a marker to visualize micrometastases in live tissue. GFP has been used as a fusion tag to monitor protein localization within living cells (16). To use GFP as a marker for *in vivo* experiments, it is necessary to establish very stable transfectants that can express GFP long-term under nonselective conditions. Previous studies have shown that retroviral transfer of the *GFP* gene can result in stable transfectants of human cancer cells *in vitro* (17). However, to study metastasis in the animal, we did not wish to add the variable of a retrovirus to the cancer cells. Therefore, a dicistronic GFP plasmid was transfected into CHO cells using liposome-mediated transfection (lipofection) for the studies described in this report. The pED-mtx^r vector (14) uses a putative internal ribosomal entry site derived from the encephalomyocarditis virus. Insertion of the *GFP* gene upstream of the internal ribosomal entry site to produce a dicistronic mRNA does not reduce the translation of the *DHFR* gene that was inserted downstream of it. The transfectants must amplify not only *DHFR* but also the *GFP* during MTX selection because of the dicistronic structure. With this plasmid, we could isolate a very stable GFP high expression CHO subclone (Fig. 1a). Furthermore, the stable GFP transfectant, Clone-38, was also stable *in vivo*, even in the absence of MTX (Fig. 1, b and c; Table 2).

To study tumor progression and the metastatic process at the earliest stages, it is important to use a metastatic model that could allow spontaneous metastasis in the animal. In the last 10 years, it has become clear that orthotopic sites of implantation are critical for the metastatic expression of transplanted tumors in nude mice. We have found that the use of tissue fragments rather than dispersed cells allows full expression of the metastatic capability of orthotopically implanted tumors (18). In the present study, *GFP* gene-transfected CHO cells were successfully used to visualize extensive peritoneal seeding as well as distant macro- and micrometastases in nude mice,

including the lung, following surgical orthotopic implantation in the ovary of s.c. tumor fragments. This model provided the opportunity to demonstrate the capability of GFP for detection and visualization of metastases.

In previous studies, the *lacZ* gene was transfected into mammalian cells to detect micrometastasis (1, 2). However, detection of *lacZ* requires extensive histological preparation and results in a high background due to endogenous β -galactosidase activity in certain cells (19). In contrast, GFP fluorescence does not need any preparation and can be seen in fresh tissues without interference from endogenous GFP. Our findings show that the screening of micrometastasis can be done easily and quickly in all systemic organs. Furthermore, using confocal microscopy with GFP transfectants, the progression of micrometastasis can be observed as seeded cells develop into a colony within relevant target organs. We have observed in these studies that as a metastatic lesion progresses and grows, the packing density of the colonies decreases (Fig. 2i). This finding suggests that development of the interstitial tissue, including angiogenesis, is an important trigger for the expansion of metastatic colonies (20). These are among the major advantages of using GFP over the other reporter genes, such as the *lacZ*, to monitor metastasis. We demonstrate here that tumor cells can be visualized in their natural state in relevant metastatic organs as has been done with intravital microscopy (21).

For an *in vivo* study of tumor progression at the single-cell level, the GFP transfectants were injected into a nude mouse i.v. Fig. 3 demonstrates the ability to detect and visualize, at the single-cell level, tumor emboli or seeding by fluorescence in the fresh tissues and blood vessels. This finding shows that GFP transfectants should also be useful with new techniques such as intravital videomicroscopy, which previously involved labeling tumor cells with dyes (21). A previous study also described the seeding and migration of mouse tumor cells externally labeled with the fluorescent dye DiI C18 in host mouse lung tissue in three-dimensional histoculture (22). However, tumor cells tagged with dyes lose their fluorescence after only a few generations and are, therefore, not useful for the long term needed to study metastasis. In contrast, GFP transfectants can be followed in the primary and target organs, because the fluorescence gene has been integrated and is passed on to subsequent generations.

Using the methods developed in the present study, GFP fluorescence will facilitate the understanding of tumor progression including micrometastasis seeding and target organ colonization, which should provide new insights into metastatic mechanisms in the patient.

ACKNOWLEDGMENTS

The authors thank Dr. R. J. Kaufman (Howard Hughes Medical Institute, University of Michigan, Ann Arbor, MI) and Genetics Institute (Cambridge, MA) for providing the pED-mtx^r vector.

REFERENCES

1. Lin, W. C., Pretlow, T. P., Pretlow, T. G., and Culp, L. A. Bacterial *lacZ* gene as a highly sensitive marker to detect micrometastasis formation during tumor progression. *Cancer Res.*, 50: 2808–2817, 1990.
2. Lin, W. C., and Culp, L. A. Altered establishment/clearance mechanisms during experimental micrometastasis with live and/or disabled bacterial *lacZ*-tagged tumor cells. *Invasion Metastasis*, 12: 197–209, 1992.
3. Morin, J., and Hastings, J. Energy transfer in a bioluminescent system. *J. Cell Physiol.*, 77: 313–318, 1972.
4. Chalfie, M., Tu, Y., Euskirchen, G., Ward, W. W., and Prasher, D. C. Green fluorescent protein as a marker for gene expression. *Science (Washington DC)*, 263: 802–805, 1994.
5. Cheng, L., Fu, J., Tsukamoto, A., and Hawley, R. G. Use of green fluorescent protein variants to monitor gene transfer and expression in mammalian cells. *Nat. Biotechnol.*, 14: 606–609, 1996.
6. Prasher, D. C., Eckenrode, V. K., Ward, W. W., Prendergast, F. G., and Cormier, M. J. Primary structure of the *Aequorea victoria* green-fluorescent protein. *Gene (Amst.)*, 111: 229–233, 1992.

7. Yang
8. Cody
9. Hein
10. Dela
11. Red-
12. Cor
13. Zol
14. Kau
15. stab
16. leac
17. 199

7. Yang, F., Miss, L. G., and Phillips, G. N., Jr. The molecular structure of green fluorescent protein. *Nat. Biotechnol.*, **14**: 1252-1256, 1996.
8. Cody, C. W., Prasher, D. C., Welstler, V. M., Prendergast, F. G., and Ward, W. W. Chemical structure of the hexapeptide chromophore of the *Aequorea* green fluorescent protein. *Biochemistry*, **32**: 1212-1218, 1993.
9. Heim, R., Cubitt, A. B., and Tsien, R. Y. Improved green fluorescence. *Nature (Lond.)*, **373**: 663-664, 1995.
10. Delagrave, S., Hawtin, R. E., Silva, C. M., Yang, M. M., and Youvan, D. C. Red-shifted excitation mutants of the green fluorescent protein. *BioTechnology*, **13**: 151-154, 1995.
11. Cormack, B., Valdivia, R., and Falkow, S. FACS-optimized mutants of green fluorescent protein (GFP). *Gene (Amst.)*, **173**: 33-38, 1996.
12. Cramer, A., Whitehorn, E. A., Tate, E., and Stemmer, W. P. C. Improved green fluorescent protein by molecular evolution using DNA shuffling. *Nat. Biotechnol.*, **14**: 315-319, 1996.
13. Zolotukhin, S., Potter, M., Hauswirth, W. W., Guy, J., and Muzycka, N. A. "Humanized" green fluorescent protein cDNA adapted for high-level expression in mammalian cells. *J. Virol.*, **70**: 4646-4654, 1996.
14. Kaufman, R. J., Davies, M. V., Wasley, L. C., and Michnick, D. Improved vectors for stable expression of foreign genes in mammalian cells by use of the untranslated leader sequence from EMC virus. *Nucleic Acids Res.*, **19**: 4485-4490, 1991.
15. Fu, X., and Hoffman, R. M. Human ovarian carcinoma metastatic models constructed in nude mice by orthotopic transplantation of histologically-impact patient specimens. *Anticancer Res.*, **13**: 283-286, 1993.
16. Gerdes, H. H., and Kaether, C. Green fluorescent protein: applications in cell biology. *FEBS Lett.*, **389**: 44-47, 1996.
17. Levy, J. P., Muldoon, R. R., Zolotukhin, S., and Link, C. J., Jr. Retroviral transfer and expression of a humanized, red-shifted green fluorescent protein gene into human tumor cells. *Nat. Biotechnol.*, **14**: 610-614, 1996.
18. Hoffman, R. M. Orthotopic is orthodox: why are orthotopic-transplant metastatic models different from all other models? *J. Cell. Biochem.*, **56**: 1-3, 1994.
19. Zdenek, L. Indigogenic methods for glycosidases. I. An improved method for β -galactosidase and its application to localization studies of the enzymes of the intestine in other tissues. *Histochemie*, **23**: 289-294, 1970.
20. Holmgren, L., O'Reilly, M. S., Folkman, J. Dormancy of micrometastases: balanced proliferation and apoptosis in the presence of angiogenesis suppression. *Nat. Med.*, **1**: 149-153, 1995.
21. Chambers, A. F., MacDonald, I. C., Schmidt, E. E., Koop, S., Morris, V. L., Khokha, R., and Groom, A. C. Steps in tumor metastasis: new concepts from intravital videomicroscopy. *Cancer Metastasis Rev.*, **14**: 279-301, 1995.
22. Margolis, L. B., Glushakova, S. E., Baibakov, B. A., Collin, C., and Zimmerberg, J. Confocal microscopy of cells implanted into tissue blocks: cell migration in long-term histocultures. *In Vitro Cell. Dev. Biol.*, **31**: 2211-2216, 1995.